Localized Pd Overgrowth on Cubic Pt Nanocrystals for Enhanced Electrocatalytic Oxidation of Formic Acid

Hyunjoo Lee[†‡], Susan E. Habas[‡], Gabor A. Somorjai[‡], and Peidong Yang[‡]

Department of Chemical Engineering, Yonsei University, Seoul, South Korea, Department of Chemistry, University of California, Berkeley, California 94720, USA, and Materials Sciences Division, Lawrence Berkeley National Laboratory, Berkeley, California 94720, USA

Email: p_yang@uclink.berkeley.edu

RECEIVED DATE ;

Single crystalline surface such as (100), (111), (110) has been studied as an idealized platform for electrocatalytic reactions since the atomic arrangement affects a catalytic property. The secondary metal deposition on these surfaces also alters the catalytic property often showing improvement such as poisoning decrease. On the other hand, electrocatalysts used for practical purpose usually have a size on the order of nanometers. Therefore, linking the knowledge from single crystalline studies to nanoparticle catalysts is of enormous importance. Recently, the Pt nanoparticles which surface structure was preferentially oriented was synthesized and used as electrocatalysts[12]. Here, we demonstrate a rational design of a binary metallic nanocatalyst based on the single crystalline study.

Clavilier et al. studied the electro-oxidation of formic acid for Pd adsorbed on Pt(100) single crystal surfaces.[5] They observed that the presence of adsorbed palladium on Pt(100) decreases self-poisoning and lowers the oxidation potential considerably. The multi-metallic nanoparticle catalysts, however, were usually prepared by co-precipitation[6] or electrodeposition[7], and control over surface structure was not achieved. We present the synthesis and application of binary Pt/Pd nanoparticles in which Pd decorates the well-defined surface of Pt nanoparticles. Pt nanocubes fully bound by (100) surfaces acted as seeds for overgrowth of Pd. Overgrowth was observed at multiple points on each seed, predominantly at the corners. Electro-oxidation of formic acid performed on these binary Pt/Pd catalysts showed the same effects of less poisoning and lower oxidation potential expected from the single crystal study.

Preparation of metal nanoparticles with shape control has often been achieved by controlling growth rates on different facets through interactions with surface-stabilizing agents.[8] However, since the catalytic activity is hindered by these surface-stabilizing agents,[9] preserving the catalytic activity of the metal surface is crucial. In this study, we used tetradecyltrimethylammonium bromide (TTAB) as a surface-stabilizing agent since it has a weak interaction with metal surfaces[9a]. The cubic Pt nanoparticles used as seeds were prepared by reducing K_2PtCl_4 dissolved in aqueous TTAB solution with $NaBH_4$ as previously reported.[9a] A TEM image of the cubic Pt seed particles is shown in Figure S1(a). Pd was nucleated on the surface of cubic Pt seeds upon reduction of K_2PdCl_4 by ascorbic acid in the presence of TTAB (See Supporting Information for more details). Figure 1(a) shows a low magnification TEM image of the binary Pt/Pd nanoparticles. Single, double and multiple nucleation of Pd on Pt nanoparticles was observed with nucleation occurring primarily on the corners. High resolution TEM images in Figures 1(b) show the interface of

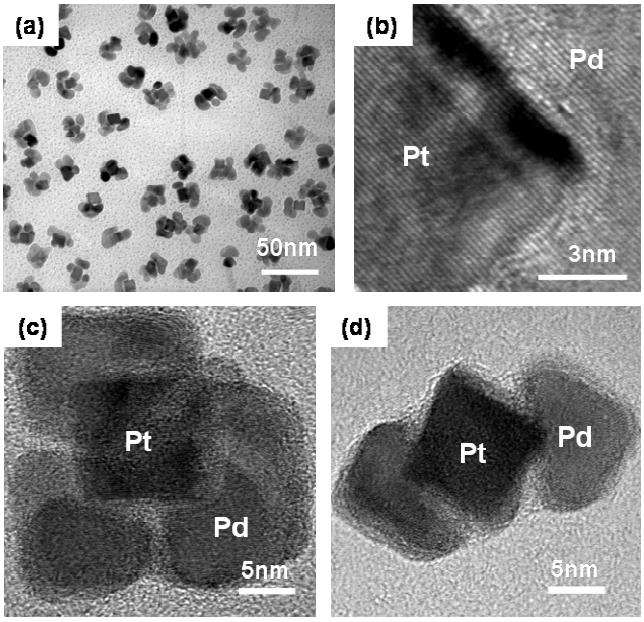

Figure 1. TEM images of (a) binary Pt/Pd nanoparticles, HR-TEM images of (b) Pt/Pd interface with an atomic resolution, (c) high Pd coverage and (d) low Pd coverage of binary Pt/Pd nanoparticles.

the two metals more clearly. Pd grew on Pt surface epitaxially. Figure 1(c) and (d) show a high and low coverage of Pd on Pt surface. The formation of multiple nucleation sites of Pd on the Pt seeds rather than conformal overgrowth depends on the rate of reduction which was controlled through pH. The addition of as-made Pt seeds (pH~9) also introduces the strongly basic metaborate ion (BO_2^-) formed during the reaction of $NaBH_4$ with water. The higher pH increases the rate of Pd reduction, probably due to better stabilization of the oxidized form of the ascorbic acid. The increased rate of reduction may encourage the formation of multiple nucleation sites rather than the conformal overgrowth of a thin Pd shell which was observed when the Pt seeds were acidified to a neutral pH[10]. The addition of base to bring the pH of the seed solution back to ~9 once again allows for the formation of multiple nucleation sites. Fully grown cubic Pd nanoparticles with a cubic Pt seed inside, shown in Figure S1(b), were prepared by decreasing the concentration of Pt seeds along with the pH. This type of epitaxial overgrowth was demonstrated previously.[12] While both the Pt and Pd surfaces are accessible on the binary Pt/Pd nanoparticles, only the Pd surface is available on the core-shell Pt/Pd nanocubes. Pd nanoparticles without Pt seeds were also prepared as shown in Figure S1(c) for comparison.

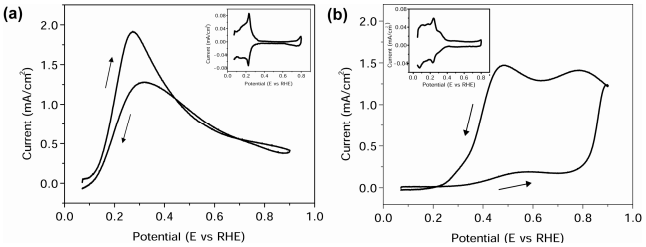

Figure 1. Cyclic voltammetric curves for (a) binary Pt/Pd nanoparticles (b) Pt nanocubes in 0.25M HCOOH + 0.5M H_2SO_4 solution at a scan rate of 50mV/s. The insets show blank voltammograms of the same electrodes in 0.5M H_2SO_4 at 50mV/s.

Each type of nanoparticle, described above, was tested for formic acid oxidation. A washed and concentrated nanoparticle solution was deposited on a Au electrode and dried at room temperature. The presence of the stabilizing agents on the nanoparticle surface required measurement of the actual surface area that was accessible for reaction. The surface areas were estimated from H adsorption/desorption cyclic voltammograms (CV) taken in sulfuric acid solution, and the results for formic acid oxidation were normalized by the estimated surface areas. Clavilier et al. reported that no oxidation was observed in the positive sweep for a Pt(100) single crystal surface and a lower oxidation peak potential was observed when Pd was adsorbed on Pt(100) (0.23V for Pd-adsorbed on Pt(100) and 0.42V for Pt(100))[5]. Under the same electrocatalytic conditions of 0.25M HCOOH+0.5M H_2SO_4 at the scan rate of 50mV/s, the CVs of the nanoparticles were collected. Figure 2 shows the CVs for (a) binary Pt/Pd nanoparticles and (b) Pt nanocubes. The insets provide blank CVs for the same sample in 0.5M H_2SO_4 solution without the formic acid. CVs for core-shell Pd nanocubes and Pd nanoparticles synthesized without Pt seed were also shown in Figure S2(a) and S2(b), respectively. The H adsorption/desorption curves for Pt cubes and Pd cubes corresponds well with the CVs for clean (100) surfaces. The binary Pt/Pd nanoparticles show an intermediate blank CV of Pt cubes and Pd cubes implying that both the Pt and Pd surface are accessible for the reaction.

In the case of the Pt cubes, the reaction is so strongly hindered by the spontaneous formation of poisoning intermediates that only minimal oxidation is observed in the positive scan[5]. Oxidation on Pt cubes only occurs in the reverse scan after the poison formed in the low range was oxidized and eliminated from the surface above 0.8V. On the other hand, no inhibition is observed in the positive scan for the binary Pt/Pd nanoparticles. Also, oxidation occurs at a much lower potential range (nearly 0.2V less) than that observed for Pt cubes (0.27V for binary Pt/Pd nanoparticles and 0.48V for Pt cubes). The presence of Pd on the surface of the Pt cubes prevents the poisoning in the positive scan and induces a considerable decrease in the activation energy for formic acid oxidation compared with Pt cubes. Oxidation of formic acid on Pd cubes and Pd nanoparticles synthesized without Pt seeds was also performed as a comparison. In both cases, no inhibition was observed in the positive scan while the peak oxidation potentials were as high as or even higher than that for Pt cubes (0.45V for the Pd cubes containing a Pt seed, and 0.52V for pure Pd particles).

Pt is known to exhibit a dual path mechanism for the oxidation of formic acid. Direct dehydrogenation produces CO_2 and H_2, while dehydration produces CO and H_2O. The evolved CO acts as a self-poisoning intermediate. We performed the CO stripping and the CV curves demonstrated that the CO stripping peak is shifted towards a higher potential for the binary Pt/Pd nanoparticles compared to the Pt cubes, while the Pd cubes and Pd nanoparticles synthesized without Pt seeds showed even higher CO stripping potentials (See Figure S3). Although a higher CO stripping potential indicates a lower CO tolerance, binary Pt/Pd nanoparticles show little deactivation in the positive scan. Therefore, only direct dehydrogenation path producing CO_2 and H_2 seems to occur when Pd is adsorbed on Pt surface, which is also observed by other research groups[11]. Also, it was shown that formic acid oxidation on Pt follows dehydration pathway at low potential producing CO[3b]. The minimized CO formation at low potential might enable to lower the peak potential for binary Pt/Pd nanoparticles.

Binary Pt/Pd nanoparticles were synthesized by localized overgrowth of Pd on cubic Pt seeds for investigation of electrocatalytic formic acid oxidation. The binary particles exhibit much less self-poisoning relative to Pt nanocubes and the lower activation energy, and these results are consistent with the single crystal study.

Acknowledgment. This work was supported by the Director, Office of Science, Office of Basic Energy Sciences, Materials Sciences and Engineering Division, of the U.S. Department of Energy under Contract No. DE-AC02-05CH1123. We thank the National Center for Electron Microscopy for the use of their facilities.

Supporting Information Available: Details for synthesis, characterization, and electrocatalytic measurements. This material is available free of charge via Internet at http://pubs.acs.org

1. Davis, S. M.; Zaera, F.; Somorjai, G. A. *J. Catal.* **1984**, *85*.
2. Bratlie, K. M.; Lee, H.; Komvopoulos, K.; Yang, P.; Somorjai, G. A. *Nano Letters* **2007**, *7*, *3097*.
3. (a) Zhou, W. P.; Lewera, A.; Larsen, R.; Masel, R. I.; Bagus, P. S.; Wieckowski, A. *J. Phys. Chem. B* **2006**, *110*, 13393-13398. (b) Arenz, M.; Stamenkovic, V.; Schmidt, T. J.; Wandelt, K.; Ross, P. N.; Markovic, N. M. *Phys. Chem. Chem. Phys.* **2003**, *5*, 4242-4251.
4. (a) Baldauf, M.; Kolb, D. M. *J. Phys. Chem.* **1996**, *100*. (b) Hoshi, N.; Kida, K.; Nakamura, M.; Nakada, M.; Osada, K. *J. Phys. Chem. B* **2006**, *110*, 12480-12484. (c) Vidal-Iglesias, F. J.; Solla-Gullon, J.; Herrero, E.; Aldaz, A.; Feliu, J. M. *Journal of Applied Electrochemistry* **2006**, *36*, 1207-1214.
5. Llorca, M. J.; Feliu, J. M.; Aldaz, A.; Clavilier, J. *Journal of Electroanalytical Chemistry* **1994**, *376*, 151-160.
6. (a) Chen, W.; Kim, J.; Sun, S.; Chen, S. *Phys. Chem. Chem. Phys.* **2006**, *8*, 2779-2786. (b) Ye, H.; Crooks, R. M. *J. Am. Chem. Soc.* **2007**, *129*, 3627-3633.
7. Jayashree, R. S.; Spendelow, J. S.; Yeom, J.; Rastogi, C.; Shannon, M. A.; Kenis, P. J. A. *Electrochimica Acta* **2005**, *50*, 4674-4682.
8. (a) Jingyi Chen, T. H. Y. X. *Angewandte Chemie International Edition* **2005**, *44*, 2589-2592. (b) Teng, X.; Yang, H. *Nano Lett.* **2005**, *5*, 885-891.
9. (a) Lee, H.; Habas, S. E.; Kweskin, S.; Butcher, D.; Somorjai, G. A.; Yang, P. *Angewante Chemi International Edition* **2006**, *45*, 7824-7828. (b) Song, H.; Rioux, R. M.; Hoefelmeyer, J. D.; Komor, R.; Niesz, K.; Grass, M.; Yang, P.; Somorjai, G. A. *J. Am. Chem. Soc.* **2006**, *128*, 3027-3037.
10. Habas, S. E.; Lee, H.; Radmilovic, V.; Somorjai, G. A.; Yang, P. *Nature Materials* **2007**, *6*, 692-697.
11. Babu, P. K.; Kim, H. S.; Chung, J. H.; Oldfield, E.; Wieckowski, A. *J. Phys. Chem. B* **2004**, *108*, 20228-20232.
12. (a) Solla-Gullon, J.; Vidal-Iglesias, F. J.; Rodfriguez, P.; Herrero, E.; Feliu, J. M.; Clavilier, J.; Aldaz, A. *J. Phys. Chem. B.* **2004**, *108*, 13573-13575. (b) Tian, N.; Zhou, Z. Y.; Sun, S. G.; Ding, Y.; Wang, Z. L. *Science* **2007**, *316*, 732-735.